Noncollinear magnetism of Cr and Mn nanoclusters on Ni(111): Changing the magnetic configuration atom by atom

Samir Lounis,* Phivos Mavropoulos, Rudolf Zeller, Peter H. Dederichs, and Stefan Blügel
Institut für Festkörperforschung, Forschungszentrum Jülich, D-52425 Jülich, Germany
(Received 22 August 2006; revised manuscript received 9 March 2007; published 24 May 2007)

The Korringa-Kohn-Rostoker Green-function method for noncollinear magnetic structures was applied on Mn and Cr nanoclusters deposited on the Ni(111) surface. We consider various dimers, trimers, and tetramers. We obtain collinear and noncollinear magnetic solutions, brought about by the competition of antiferromagnetic interactions. It is found that the triangular geometry of the Ni(111) substrate, together with the intracluster antiferromagnetic interactions, is the main cause of the noncollinear states, which are secondarily affected by the cluster-substrate exchange interactions. The stabilization energy of the noncollinear, compared to the collinear, states is calculated to be typically of the order of 100 meV/atom, while multiple local-energy minima are found, corresponding to different noncollinear states, differing typically by 1–10 meV/atom. Open structures exhibit sizable total moments, while compact clusters tend to have very small total moments, resulting from the complex frustration mechanisms in these systems.

DOI: 10.1103/PhysRevB.75.174436 PACS number(s): 75.75.+a, 36.40.Cg, 75.30.Hx, 73.22.−f

I. INTRODUCTION

Future technologies will be based on the magnetic properties of nanostructures. Such magnetic structures can be composed of magnetic atoms in precise arrangements. The magnetic properties of each atom can be profoundly influenced by its local environment, and size-selected nanoclusters can show complex magnetic behavior, with moments changing nonmonotonically with the number of atoms.[1] Recently, Gambardella *et al.*[2] showed that Co adatoms on Pt(111) have giant magnetic anisotropy energy (MAE) which may open the way to very high data storage densities. Indeed, clusters have the potential of increasing the density in information storage. One may envision that future magnetic hard discs with information carried by magnetic clusters will have a storage density two orders of magnitude larger than those used today. Here we show, for elements without high MAE, i.e., adatoms with half filled three-dimensional (3d) shells (Cr and Mn), that the magnetic properties due to the competition of antiferromagnetic (AF) exchange coupling may be used to switch the moment configuration in small adclusters, from high-moment collinear to low-moment noncollinear. The mechanism is based on the response of the magnetic state of an adcluster to the exchange field of an adjacent adatom, which can be attached to or removed from the cluster, e.g., by a scanning tunneling microscope (STM) tip. In fact, Jamneala *et al.*[3] investigated by STM Cr trimers deposited on Au(111). They show that moving a Cr adatom of a compact trimer leads to a switching from the Kondo state to a magnetic one. This may reach an important goal for a magnet's storage capability: the bit 0 can be considered when no (or very small) magnetic moment is measured while a high magnetic moment of the cluster can be considered as 1.

Magnetic excitations may degrade the performance of high-density memories. Indeed, using scanning tunneling microscopy (STM) Heinrich *et al.*[4] could elucidate the spin flip of individual magnetic atoms that are dispersed on a non magnetic matrix. Therefore we also discuss the energetic stability of the high-moment collinear and low-moment, noncollinear states.

Recently, there has been increasing interest in investigating noncollinear nanostructures on ferromagnetic[5–7] or nonmagnetic surfaces.[8–12] Here, we choose as a substrate a ferromagnetic (FM) fcc-Ni surface which provides a magnetic coupling between the adatoms and the substrate atoms. The Ni(111) surface was chosen, in which the surface geometry is triangular, meaning, in terms of magnetic coupling,[8] that a compact trimer with antiferromagnetic interactions sitting on the surface necessarily suffers magnetic frustration. This frustration leads to the well-known noncollinear Néel states being characterized by 120° angles between the moments. Hence in such a system we face an interplay between the noncollinear coupling tendencies arising from the interaction among the adatoms in the cluster and the collinear tendencies arising from the additional coupling to the substrate atoms. This is very different from the Ni(001) surface where the frustration and noncollinear state arises from the competition between the coupling in the cluster and with the substrate.[5]

II. CALCULATIONAL METHOD

Our calculations are based on the local spin-density approximation[13] (LSDA) of density-functional theory with the parametrization of Vosko *et al.*[14] The full nonspherical potential was used, taking into account the correct description of the Wigner-Seitz atomic cells.[15,16] Angular momenta up to $l_{\max}=3$ were included in the expansion of the Green functions and up to $2l_{\max}=6$ in the charge-density expansion. Relativistic effects were described in the scalar relativistic approximation.

First, the surface Green functions are determined by the screened Korringa-Kohn-Rostoker (KKR) method[17] for the (111) surface of Ni which serves as the reference system. The LSDA equilibrium lattice parameter of Ni was used (6.46 a.u.$\approx$3.42 Å) and the magnetic moment at the surface is $0.63\mu_B$. Within the KKR method, the Green function of the perturbed sites (here the adcluster and a few neighboring

shells of the host) is connected to the surface Green function via a Dyson equation.[5] Thus the boundary conditions of the ideal surface are included, and no artificial periodic supercell is needed for the description of a single adcluster. To describe the Cr and Mn adatoms on the surface we consider a cluster of perturbed potentials with a size of 48 perturbed sites for all kinds of adclusters considered. In all cases, the 48 perturbed sites include at least one shell of first neighboring sites of the adcluster atoms. Total-energy calculations are done[18] by using Lloyd's formula (a generalization of the Friedel sum rule), which takes into account the contribution of the Friedel oscillations up to infinity in a semianalytical way. Tests have shown[18] that the use of Lloyd's formula gives a very fast convergence of the total energy with respect to the number of surrounding perturbed shells, already in the sub-meV range for one shell.

We consider the adatoms at the unrelaxed hollow position in the first vacuum layer. We allow for the relaxation of the magnetic moment directions with respect to the direction of the substrate magnetization.[5]

Spin-orbit coupling and dipole-dipole magnetic interactions are not included in our calculations. Under these conditions, spin space and real space are decoupled, and the orientation of the magnetic moments can be rotated by an arbitrary angle, as long as this rotation is the same for all moments (including those of the Ni surface). Therefore our results on the orientations must be considered to be relative to the orientation of the substrate moment, which we take as a reference, and which depends on numerous details specific to an experiment, such as the Ni film thickness, external magnetic fields for an appropriate orientation of the moments during measurement, etc. Our study is devoted to the local electronic structure in the vicinity of the cluster, and the substrate magnetization is taken in the figures to point out-of-plane for illustrative purposes.

In the self-consistent calculations we tried several initial configurations, which ended up in the local-energy minima presented here. The full phase space cannot be scanned densely, since it would require 1000 self-consistency calculations even for a moderate number of ten different directions per atom in a trimer. Thus we searched for local minima guided by symmetry considerations.

III. THEORETICAL BACKGROUND

Since the collinear magnetic state represents a self-consistent solution of the Kohn-Sham equations, total-energy calculations are necessary to check whether the noncollinear solution represents a true energy minimum or only a local minimum, with the collinear state representing the total minimum. This proved to be important, e.g., for Cr dimers on Ni(001),[5] where the collinear solution was found to have a lower total energy.

The driving mechanism for noncollinear magnetism in small transition-metal clusters is a competition of antiferromagnetic (or antiferromagnetic and ferromagnetic) interactions. In other cases, such as *f*-element systems[19] or adlayers and chains,[20,21] the spin-orbit interaction can also be of significance but in transition metals usually frustration is the dominating effect. In the case of magnetically noncollinear transition metal clusters adsorbed on ferromagnetic surfaces, it is helpful for the interpretation of the results to distinguish between three factors contributing to the solution: (i) the magnetic interaction of the cluster adatoms with the substrate, (ii) the magnetic pair interaction among the atoms in the cluster, and (iii) the geometry of the cluster. This separation is meaningful because the first-neighbors exchange interaction is energetically dominant compared to second, third, etc., neighbors, and because in different cluster sizes or shapes the type of pair interaction (ferro- or antiferromagnetic) does not change qualitatively. Quantitatively, however, this is only an approximation, and effects beyond this are included in the self-consistent solution. In view of the above, we proceed by first presenting results for the single adatoms, then the dimers, and then trimers and tetramers of various shapes. We expect that Cr and Mn clusters are candidates for noncollinear magnetism, because the Cr-Cr and Mn-Mn first-neighbors pair interactions are antiferromagnetic.

IV. SINGLE ADATOMS AND DIMERS

Investigating the magnetism of adclusters starts by understanding the magnetism of adatoms and addimers.

Single adatoms. Our calculations show that the single Cr adatom is antiferromagnetically coupled to the surface with an increase of the magnetic moments ($M_{\mathrm{AF}}=3.77\mu_B$ and $M_{\mathrm{FM}}=3.70\mu_B$) compared to the results obtained for Ni(001)[5] ($M_{\mathrm{AF}}=3.48\mu_B$ and $M_{\mathrm{FM}}=3.35\mu_B$). This increase arises from the weaker hybridization of the 3d wave functions with the substrate—the adatom has three neighbors on the (111) surface and four on the (001). The calculated energy difference between the FM and AF configurations is high so that the AF configuration is stable at room temperature ($\Delta E_{\mathrm{AF-FM}}=-93.54$ meV, corresponding to 1085 K). Also our results for the Mn adatom on Ni(111) are similar to what we found on Ni(001). The single Mn adatom prefers to couple ferromagnetically to the substrate. The energy difference between the two possible magnetic configurations is $\Delta E_{\mathrm{AF-FM}}=208$ meV. For the (001) surfaces the energy differences are both for Cr and Mn larger, since they roughly scale with the coordination number ($\Delta E^{\mathrm{Cr}}_{\mathrm{AF-FM}}=-134$ meV, $\Delta E^{\mathrm{Mn}}_{\mathrm{AF-FM}}=252$ meV). The magnetic moments of Mn are high and reach a value of $4.17\mu_B$ for the FM configuration and $4.25\mu_B$ for the AF configuration. The moments are higher than for the Mn adatoms on Ni(001) ($M_{\mathrm{AF}}=4.09\mu_B$ and $M_{\mathrm{FM}}=3.92\mu_B$), again due to the lower coordination and hybridization of the 3d levels. This type of coupling to the substrate (AF for Cr and FM for Mn) can be understood in terms of the *d-d* hybridization of the adatom wave functions with the ones of the substrate, and is described, e.g., in Ref. 5.

Dimers. For the compact dimers, three collinear configurations are possible: ferromagnetic (FM) [see Fig. 1(a)], with the moments of both atoms parallel to the substrate moments , antiferromagnetic (AF) [Fig. 1(b)], with the moments of both atoms antiparallel to the substrate moments, and ferrimagnetic (Ferri) [see Fig. 1(c)], where the magnetic moment of one of the dimer atoms is parallel to the moments of the substrate, while the other one is antiparallel. Since the direct

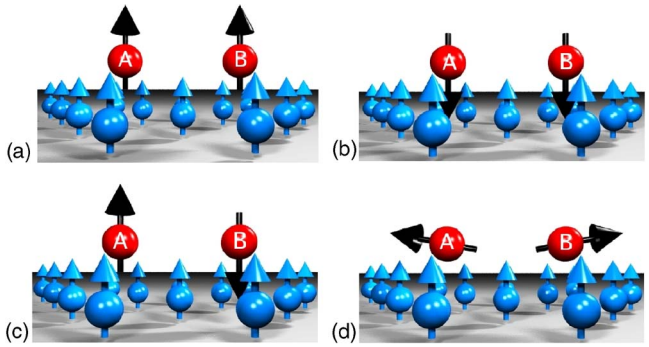

FIG. 1. (Color online) Different magnetic configurations of Mn dimer on Ni(001). The Mn atoms are labeled by A and B; unlabeled atoms (in blue or light gray) correspond to the Ni substrate. The configurations correspond to FM in (a), AF in (b), Ferri in (c) which is the ground state, and the noncollinear additional local minimum in (d). See text for the discussion.

exchange in a Cr pair (or a Mn pair) is antiferromagnetic (for an explanation in terms of the Alexander-Anderson model[22] see Ref. 5), and stronger than the adatom-substrate interaction, the Ferri solution is expected to prevail. Indeed, Cr dimers on Ni(111) as on Ni(001) are characterized by a collinear Ferri coupling as a ground state. The difference is, however, that no noncollinear solution was found on Ni(111), as opposed to Ni(001).[5] This is understandable, because the noncollinear state in the dimer on Ni(001) arises from the competition between the intradimer Cr-Cr antiferromagnetic interaction and the Cr-Ni antiferromagnetic interaction. On the Ni(111) surface, the coordination to the Ni substrate is lower, therefore the interaction with the substrate is insufficient to overcome the Cr-Cr interaction. In fact, the Ferri total energy is 317.32 meV/adatom lower than the AF one and 352.54 meV/adatom lower than the FM one.

Similar trends are found for the Mn dimers on Ni(111): the Ferri solution is the most stable collinear solution. However, in addition, a noncollinear solution is found, which is only slightly higher, i.e., by 4.44 meV/adatom than the Ferri solution. Note that on the Ni(001) surface,[5] this type of dimer state, shown in Fig. 1(d), represents the ground state, which is, however, not the case for the dimer on (111) preferring the Ferri configuration. In the noncollinear configuration [Fig. 1(d)], both adatom moments ($3.90\mu_B$), while

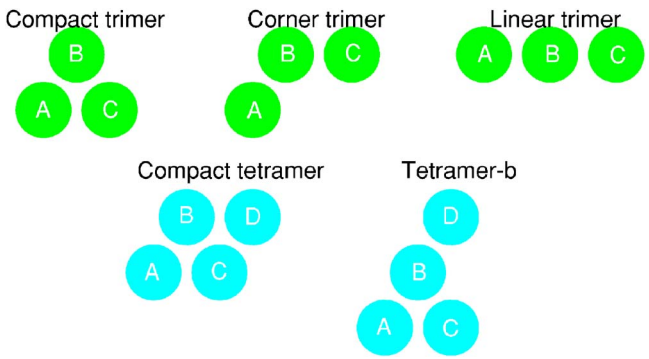

FIG. 2. (Color online) Different geometrical configurations considered for trimers and tetramers at the surface of Ni(111).

TABLE I. Atomic spin moments (in μ_B) of the adatom dimers on Ni(111) in the collinear configurations. A minus sign of the collinear moments indicates an antiparallel orientation with respect to the substrate magnetization.

	Cr_2	Mn_2
AF moments	(−3.47, −3.47)	(−4.02, −4.02)
Ferri moments	(−3.30, 3.31)	(−3.97, 3.85)
FM moments	(3.38, 3.38)	(3.98, 3.98)

aligned antiferromagnetically with respect to each other, are slightly tilted in the direction of the substrate magnetization with a rotation angle of θ=79° (instead of 90°). The energy differences between the Ferri and the other local minima AF and FM are, respectively, 243.2 and 76.31 meV/adatom. The magnetic moments and energy differences are given in Tables Iand II. Note that the local Cr and Mn moments are considerably higher than the corresponding local moments in dimers on Ni(001),[5] again a result of the reduced coordination number.

As we have discussed in Ref. 5, the different magnetic configurations of the Ni substrate atoms cannot be described well by the Heisenberg model, since the moments of the atoms adjacent to the adatoms are strongly reduced. Such longitudinal moment relaxations cannot be described by this model.

V. ADATOM TRIMERS

Trimers in equilateral triangle geometry are, in the presence of antiferromagnetic interactions, prototypes for noncollinear magnetism, with the magnetic moments of the three atoms having an angle of 120° to each other.[9] This *120° configuration* is a well-known consequence of the magnetic frustration in such triangular systems. Examples are compact Cr or Mn trimers on (111) surfaces of noble metals (see, for instance, a recent calculation of Mn_3 on Cu(111) reported in Ref. 8). In our case, the 120° state is perturbed by the exchange interaction with the substrate, and therefore the magnetic configuration is expected to be more complicated.

Let us start with a Cr dimer (Mn dimer) that we approach by a single Cr adatom (Mn adatom). As shown in Fig. 2, three different types of trimers can be formed: (i) the compact trimer with an equilateral shape, (ii) the corner trimer with an isosceles shape, and (iii) the linear trimer. The adatoms are named A, B, and C.

TABLE II. Dimer energies (in meV/adatom) in the FM, AF, and Ferri configurations of Cr and Mn dimers on Ni(111). Results of the same dimers on Ni(001), taken from Ref. 5, are also shown for comparison.

Dimer type Substrate	Cr_2 Ni(111)	Cr_2 Ni(001)	Mn_2 Ni(111)	Mn_2 Ni(001)
$E_{\text{FM-Ferri}}$	353	451	76	65
$E_{\text{AF-Ferri}}$	317	433	243	496

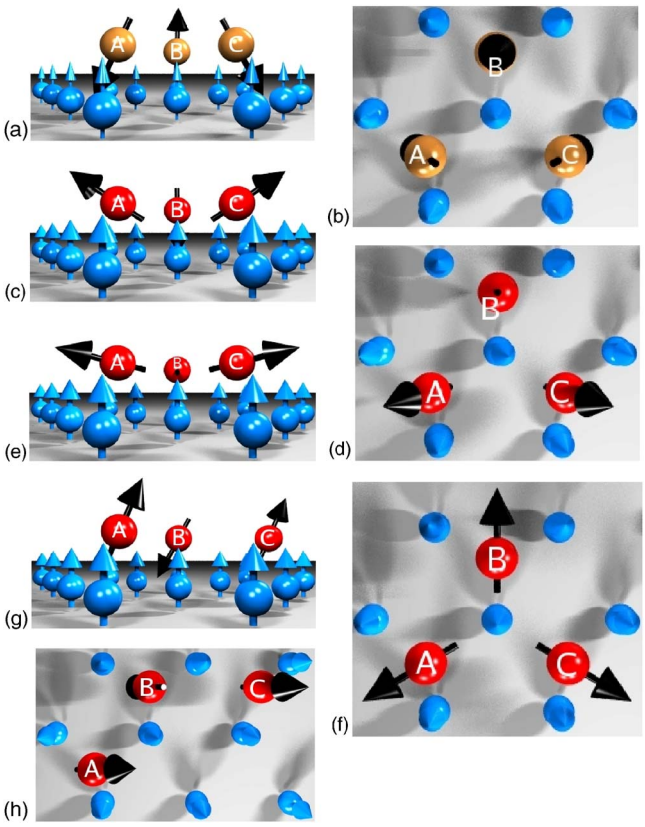

FIG. 3. (Color online) Side view (a) and top view (b) are shown for the most stable configuration of Cr compact trimer on Ni(111); this corresponds also to the NCOL1 configuration of the Mn compact trimer. (c) and (d) represent the side view and top view of the ground state (NCOL2) of Mn compact trimer on Ni(111) while (e) and (f) depict an almost degenerate state (NCOL3) of the same Mn trimer. Finally, the side view (g) and top view (h) are shown for the most stable configuration of Mn corner trimer on Ni(111). The adatoms are labeled by A, B, and C. Unlabeled atoms (in blue or light gray) correspond to the Ni substrate. See text for more details.

When the distance between the ad-dimer and the single adatom is large enough that their magnetic interaction is weak (second-neighboring positions[5]), the total moment is $-3.78\mu_B$ for the Cr case and $4.05\mu_B$ for the Mn one. Let us move the single adatom close to the dimer and form a compact trimer. The distance between the three adatoms is the same, meaning that this is a prototype geometry which leads for a trimer in free space to a 120° rotation angle between the magnetic moments. This is attested for the Cr case for which we had difficulties finding a collinear solution. Our striking result, as depicted in Figs. 3(a) and 3(b), is that the noncollinear 120° configuration is conserved with a slight modification. Indeed, our self-consistent (θ, ϕ) angles are (2°,0°) for adatom B, (126°,0°) for adatom A, and (122°,180°) for adatom C. The angle between B and A is equal to the angle between B and C (124°) while the angle between A and C is 112°. The small variation from the prototypical 120° configuration is due to the additional exchange interaction with Ni atoms of the surface. Let us suppose that we start with a 120° configuration of a compact Cr trimer, neglecting at first the exchange interaction with the substrate. This gives an infinite number of degenerate configurations being distinguished by an arbitrary rotation of all moments in spin space. This degeneracy is (partly) removed by coupling to the substrate atoms, the moments of which are fixed by anisotropy, e.g. in the [111] direction. Since the adatom-substrate interaction is AF, the moments of two adatoms rotate so that they are partly oriented opposite to the substrate magnetization, while the moment of the third adatom rotates to the opposite direction, driven by the AF interaction to its Cr neighbors. The coupling with the substrate leads thus to a deviation from the prototype 120° state, with an additional rotation of 2° for the FM adatom and of 4° for the two other adatoms. The Cr B-atom carries a moment of $2.94\mu_B$, smaller than the neighboring moments $(3.31\mu_B)$. Hence the total magnetic moment of all the adatoms is $-0.76\mu_B$. Note the huge jump of the total magnetic moment (80%) from $-3.78\mu_B$, which is the initial noninteracting dimer-adatom total moment.

For the compact Mn trimer, three noncollinear configurations were obtained: As in the case of the compact Cr trimer, the free Mn trimer must be in a 120° configuration. Nevertheless, the magnetism of the substrate changes this coupling taking into account the single adatom behavior: Mn adatoms prefer a FM coupling to the substrate and an AF coupling with their neighboring Mn adatom.

The first noncollinear magnetic configuration (NCOL1) is similar to the Cr one [Figs. 3(a) and 3(b)], i.e., adatom B couples ferromagnetically $(3.61\mu_B)$ with the substrate moments while adatom A $(3.67\mu_B)$ and C $(3.67\mu_B)$ are rotated into the opposite direction with an angle of 114° between B and A and between B and C (see Table III).

The second noncollinear configuration (NCOL2) has the opposite magnetic picture [Figs. 3(c) and 3(d)] as compared to the compact Cr trimer. Atoms A and C tend to couple ferromagnetically to the substrate, with a tilting of $\theta=49°$, $\phi=0°$ for atom A and $\theta=51°$, $\phi=180°$ for atom C; each of them carries a moment of $3.62\mu_B$. The AF interaction of atom B with A and C forces it to an AF orientation with respect to the substrate, characterized by $\theta=179°$, $\phi=0°$, and a moment of $3.70\mu_B$. Thus the trimer deviates from the 120° configuration: the angles between A and B moments and B and C moments are about 130°, and the angle between A and C is about 100°.

In the third magnetic configuration (NCOL3) the three moments $(3.65\mu_B)$ are almost in plane and perpendicular to the substrate magnetization [see Figs. 3(e) and 3(f)]. They are also slightly tilted in the direction of the substrate magnetization $(\theta=86°)$ due to the weak FM interaction with the Ni surface atoms. Within this configuration, the 120° angle between the adatoms is almost kept. Total-energy calculations show that the NCOL2 configuration is the ground state which is almost degenerate with NCOL1 and NCOL3 ($\Delta E_{\mathrm{NCOL1-NCOL2}}=1.27$ meV/adatom and $\Delta E_{\mathrm{NCOL3-NCOL2}}=5.61$ meV/adatom). Thus already at low temperatures trimers might be found in all three configurations; in fact the spin arrangement might fluctuate between these three 120° configurations or at even lower temperatures between the three degenerate configurations of the NCOL1 or the NCOL2 state. Compared to the collinear state energy of the compact trimer, the NCOL2 energy is lower by 138.23 meV/adatom.

TABLE III. Size and rotation angles of the magnetic moments of Mn adatoms forming a compact trimer on Ni(111) surface. For the adatom notation see Fig. 2. All three states are calculated to be local-energy minima. The energy difference per adatom with respect to NCOL2 is also shown. The collinear state is energetically 138.23 meV/adatom higher than NCOL2.

Noncol. config.	Adatom	Moment (μ_B)	θ	ϕ	Energy/adatom (meV)
	A	3.67	115°	0	
NCOL1	B	3.61	1°	0	1.27
	C	3.67	113°	180°	
	A	3.62	49°	0	
NCOL2	B	3.70	179°	0	0
	C	3.62	50°	180°	
	A	3.65	86°	240°	
NCOL3	B	3.65	86°	0	5.61
	C	3.65	86°	120°	

This very high-energy difference is due to frustration, even higher than breaking a bond as shown in the next paragraphs. Contrary to this, the corner trimer shows a collinear ground state because it is not frustrated. For instance, the total moment of the noncollinear compact trimer ($0.95\mu_B$) experiences a decrease of 76% compared to the obtained value for the noninteracting dimer-adatom configuration.

The next step is to move the additional adatom C and increase its distance with respect to A in order to reshape the trimer into an isosceles triangle (what we call "corner trimer" in Fig. 2, with one angle of 120° and two of 30°). By doing this, the trimer loses the frustration and is characterized thus by a collinear ferrimagnetic ground state: the moments of adatoms A and C are antiferromagnetically oriented to the substrate (following the AF Ni-Cr exchange), while the moment of the central adatom B is ferromagnetically oriented to the substrate, following the AF Cr-Cr coupling to its two neighbors. The magnetic moments do not change much compared to the compact trimer. The central adatom B carries a moment of $2.94\mu_B$ while the two others have a slightly more sizable moment of $-3.32\mu_B$. Thus the total magnetic moment ($-3.70\mu_B$) increases to a value close to the one obtained for the noninteracting dimer-adatom system.

While the noncollinear state is lost for the corner Cr trimer, it is present for the corner Mn trimer as a local minimum with a tiny energy difference of 4.82 meV/adatom higher than the Ferri ground state. This value is equivalent to a temperature of ~56 K, meaning that at room temperature both configurations co-exist. Here Ferri means that the central adatom B is antiferromagnetically oriented to the substrate with a magnetic moment of $3.71\mu_B$, forced by its two FM companions A and C (moment of $3.83\mu_B$) which have only one first neighboring adatom and are less constrained. The total moment of the adcluster is also high ($3.95\mu_B$) compared to the compact trimer value, reaching the value of the noninteracting system (with the third atom of the trimer far away from the other two).

The Ferri solution is just an extrapolation of the noncollinear solution shown in Figs. 3(g) and 3(h) (with magnetic moments similar to the collinear ones) in which the central adatom B ($3.70\mu_B$) tends to orient its moment also antiferromagnetically to the substrate ($\theta=152°$, $\phi=0°$) and the two other adatoms with moments of $3.83\mu_B$ tend to couple ferromagnetically to the surface magnetization with the same angles ($\theta=23°$, $\phi=180°$). It is important to point out that the AF coupling between these two latter adatoms is lost by increasing the distance between them. Indeed, one sees in Figs. 3(g) and 3(h) that the two moments are parallel. The total magnetic moment is also high and is equal to $3.78\mu_B$.

Let us move, furthermore, adatom C in order to form a linear trimer. For the Cr case, there is no noncollinear magnetism. The already stable Ferri solution for the corner trimer is comforted. The moments of the adatoms A and C are a bit higher than that obtained so far for the other structural configuration, i.e., adatoms A and C have a moment of $-3.40\mu_B$ while the central moment is equal to $2.97\mu_B$: the coupling between A and C is now indirect (through the central adatom). The total magnetic moment is also high ($-3.83\mu_B$).

Concerning the Mn case for a linear trimer, a noncollinear configuration was obtained as a local minimum with a small energy difference compared to the ground state which is the collinear Ferri solution (8.50 meV/adatom ~99 K). The magnetic moments do not change a lot compared to the values obtained for the corner trimer. The central adatom B carries a moment of $-3.78\mu_B$ while the A and C have a higher moment of $3.84\mu_B$. In the noncollinear solution, the central Mn adatom with a moment of $3.76\mu_B$, as seen previously, tends to couple antiferromagnetically with ($\theta=142°$, $\phi=0°$) and the A and C with a similar moment of $3.85\mu_B$ tend to couple ferromagnetically to the substrate ($\theta=28°$, $\phi=180°$). The total moment is high for both magnetic configurations. For the Ferri solution, it reaches $3.90\mu_B$, while for the noncollinear solution the total moment value is smaller ($3.84\mu_B$).

It is interesting to compare the total energies of the three trimers we investigated. The compact trimer has more first neighboring bonds and is expected to be the most stable trimer. The energy differences confirm this statement. Indeed the total energy of the Cr compact trimer is 119 meV/adatom lower than the total energy of the corner trimer and 198.16 meV/adatom lower than the total energy of the linear trimer. Similarly, the Mn compact trimer has a lower energy

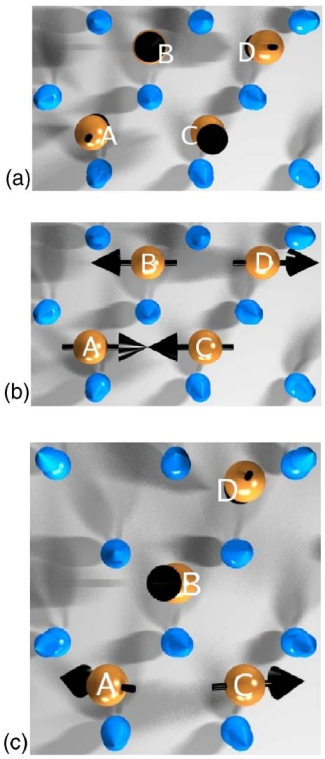

FIG. 4. (Color online) Top view of the collinear most stable solution (a) and the noncollinear metastable configuration (b) of compact Cr tetramer on Ni(111). In (c) is depicted the Cr tetramer-*b* magnetic ground state on Ni(111), which basically consists of the noncollinear trimer state of Fig. 3(a) coupled antiferromagnetically to the fourth adatom. The adatoms are labeled by A, B, C, and D. Unlabeled atoms (in blue or light gray) correspond to the Ni substrate.

of 53 meV/adatom compared to the corner trimer and a lower energy of 100 meV/adatom than the linear trimer.

Summarizing the results for the total moments of the adatoms, we see that the noninteracting cluster consisting of a single adatom and an adatom dimer has a high moment. This large total moment also survives for linear and corner trimers. However, the most stable compact trimer has a low moment, $0.95\mu_B$ in the case of Mn and $-0.76\mu_B$ for Cr.

VI. ADATOM TETRAMERS

We consider two types of tetramers, formed by adding a Cr or Mn adatom (atom D in Fig. 2) to the compact trimer. We begin with the compact tetramer [see Figs. 2, 4(a), and 4(b)]. For both elements Cr and Mn, the Ferri solution is the ground state [Fig. 4(a)]. For Cr (Mn) compact tetramer, the A and D adatoms are ferromagnetically oriented to the surface atoms with a moment of $2.31\mu_B$ ($3.60\mu_B$) while B and C are antiferromagnetically oriented to the substrate with a moment of $2.87\mu_B$ ($3.43\mu_B$). This gives a magnetic configuration with a low total magnetic moment of $-1.12\mu_B$ for the Cr tetramer and $0.34\mu_B$ for the Mn tetramer. The Cr tetramer, in particular, shows also a noncollinear configuration [Fig. 4(b)] as a local minimum which has, however, a slightly higher energy of $\Delta E_{\mathrm{NCOL-Ferri}}=1$ meV/adatom. Within this configuration the AF coupling between the adatoms is observed. However, the four moments are almost in plane perpendicular to the substrate magnetization. The tilting is small ($\theta=93°$) due to the weak AF coupling with the substrate.

An additional manipulation consists in moving the adatom D and forming a tetramer-*b* [Fig. 4(c)]. For such a structure, the collinear solution for the Cr tetramer is only a local minimum. In this structure, atom D has less neighboring adatoms compared to A, B, and C. In the noncollinear solution which is the magnetic ground state, the moment of adatom D ($3.34\mu_B$) is almost antiferromagnetically oriented to the substrate ($\theta=178°$, $\phi=0°$). The remaining adatoms form a compact trimer in which the closest adatom to D, i.e., B, tends to orient its moment ferromagnetically ($2.45\mu_B$) to the substrate ($\theta=19°$, $\phi=0°$) while the moments of A ($2.90\mu_B$) and C ($2.80\mu_B$) tend to be oriented antiferromagnetically ($\theta_A=124°$, $\phi_A=0°$) and ($\theta_C=107°$, $\phi_C=180°$). In the (metastable) collinear solution for this tetramer, the moment of adatom B is oriented ferromagnetically to the substrate while the moments of all remaining adatoms are oriented antiferromagnetically to the surface atoms. Here, the total magnetic moment has a high value of $-3.46\mu_B$. The total-energy difference between the two configurations is equal to 49.32 meV/adatom. Compared to the total energy of the compact tetramer, our calculations indicate that the tetramer-*b* has a higher energy (108.72 meV/adatom).

Let us now turn to the case of the Mn tetramer-*b*. Also here, the noncollinear solution is the ground state while the collinear one is a local minimum. The energy difference between the two solutions is very small (2.82 meV/adatom). The moments are now rotated to the opposite direction compared to the Cr case, in order to fulfill the magnetic tendency of the single Mn adatom which is FM to the substrate. The Mn atom with less neighboring adatoms, i.e., D, has a moment of $3.84\mu_B$ rotated by ($\theta=27°$, $\phi=0°$), while its closest neighbor, the atom B with a moment of $3.44\mu_B$, is forced by the neighboring companions to couple AF ($\theta=140°$, $\phi=180°$). The adatoms A and C with similar magnetic moments ($3.63\mu_B$) tend to couple ferromagnetically with the following angles: ($\theta=81°$, $\phi=0°$) and ($\theta=34°$, $\phi=0°$). As in the case of Cr tetramer-*b*, the converged collinear solution is just the extreme extension of the noncollinear one: The "central" adatom of the tetramer is forced by its FM Mn neighboring atoms to coupled antiferromagnetically to the substrate. The magnetic regime is similar to the one of Cr tetramer-*b*, i.e., high, with a total magnetic moment of $4.37\mu_B$.

As expected, the most stable tetramer is the compact one, with an energy of 52.26 meV/adatom lower than tetramer *b*.

VII. LIMITATIONS OF PRESENT CALCULATIONS

We now discuss the limitations of our calculations due to the following approximations: (i) neglect of structural optimization, (ii) neglect of spin-orbit coupling, and (iii) use of the local spin-density approximation to density-functional theory.

(i) Structural optimization can affect the results on the interatomic exchange interactions and magnetic ground state. In the case of Cr and Mn adatoms on Ni, the structural relaxations and the changes in the magnetic state are expected to be small. In order to test this, we compare the forces and exchange constants for two geometries of a magnetically collinear Mn dimer: the "unshifted," ideal crystal geometry (with the dimer atoms at the lattice positions, as was done in the rest of this work) and a "shifted" geometry, with the dimer atoms appreciably shifted towards the surface by 10.4% of the Ni(111) interplanar distance (6% of the lattice constant). In both cases, the ferrimagnetic configuration corresponds to the collinear ground state. The forces are found to be different on the two magnetically inequivalent dimer atoms. In the unshifted geometry, the forces have a perpendicular component *toward* the surface, $F_z=-16.5$ and -25 mRyd$/a_B$ (a_B is the Bohr radius), respectively corresponding to the adatom with moment parallel and antiparallel to the surface moment, and a lateral component pushing the dimer atoms apart, $F_x=24.4$ mRyd$/a_B$. In the shifted geometry, the perpendicular forces are about a factor 4 stronger, $F_z=84.9$ and 82.4 mRyd$/a_B$, pointing *away* from the surface, while the lateral forces are $F_x=30$ mRyd$/a_B$, again pushing the dimer atoms apart. We conclude that the dimer must relax toward the surface by about 2% of the interplanar distance, while the atoms will also move slightly away from each other. This is confirmed in calculations for a 2% perpendicular relaxation, giving rise to only very small perpendicular forces ($F_z=0.3$ and -4.5 mRyd$/a_B$ toward the surface). The energy difference, $\Delta E=E_{\mathrm{Ferri}}-E_{\mathrm{Ferro}}$, changes from $\Delta E=-147$ meV in the unshifted geometry to $\Delta E=-150$ meV in the 2%-shifted geometry and $\Delta E=-182$ meV in the 10.4%-shifted geometry; i.e., a 2% vertical shift induces only a 2% change in the interatomic exchange energies, while a 10% vertical shift induces a 25% change. The effect of the expected 2% relaxation (including the lateral relaxation) to the equilibrium position should therefore be small. Calculations on the Cr ferrimagnetic dimer in the unshifted geometry show forces less than 5 mRyd$/a_B$, meaning that the structural relaxation of the dimer will be very small.

In recent calculations[23] on ferromagnetic Co clusters on Au(111), the effect of interatomic spacing on the exchange interactions was tested by decreasing the lattice parameter by about 4%. It was found that such a decrease brought a change of the order of 10% in the pairwise exchange constants.

As a conclusion, our central result, namely that compact structures are in a noncollinear magnetic ground state while open structures are in a collinear state, does not change by structural relaxations. What can change, however, are the exact angles of the moments in the noncollinear state, as well as the small energy differences beteween the various noncollinear energy minima (which were of the order of a few meV).

(ii) Spin-orbit coupling is weak in these nanoclusters, because Cr and Mn atoms have a half filled *d* shell, i.e., filled spin-up shell and unfilled spin-down shell. In the past, calculations[24] on the magnetocrystalline anisotropy energy (MAE) of transition-metal adatoms on Ag and Au surfaces (where the spin-orbit coupling is strong) have shown that Cr and Mn adatoms have a MAE of less than 5 meV. On Ni, the effect should be weaker, as on Cu, where the MAE of a single Co adatom was calculated[25] to be less than 1 meV. Much stronger MAE was found,[2] e.g., for Co adatoms on Pt (MAE of the order of 10 meV) or for 5D adatoms on Ag and Au (MAE of the order of 30 meV), caused by the fact that the Fermi level is in the middle of the spin-down 3d shell of Co and by the strong spin-orbit coupling of the 5d adatoms and the Pt, Au, and Ag substrate. Moreover, as shown in Ref. 2, even the relatively strong MAE of 10 meV of the Co adatom on Pt drops rapidly with cluster size. Considering these effects, we believe that spin-orbit coupling cannot significantly affect the magnetic state of Cr and Mn adclusters on Ni.

(iii) Local approximations to density-functional theory, i.e., the LSDA (which was used here) and the generalized gradient approximation (GGA), are known to fail when electron correlations are strong. In the case of 3d adatoms and adclusters, however, hybridization with the substrate reduces the electron correlations so that local density-functional theory becomes satisfactory (except in Kondo systems). Concerning the use of LSDA instead of GGA, in the case of the small deposited clusters considered here, the magnetic moments are pronounced and the exchange interactions clear: the interaction to the substrate is weakly ferromagnetic for Mn and antiferromagnetic for Cr, and the first-neighbor, intracluster interaction is strongly antiferromagnetic. Therefore this is not a sensitive case, where the LSDA and GGA would give considerably different results. Small energy differences, of the order of 1 or 2 meV per atom (which are found comparing several noncollinear configurations) can depend on the type of functional used; however, such accuracy is beyond the predictive power of local density-functional theory (LSDA or GGA) for these systems.

VIII. SUMMARY

As a summary, we have investigated the complex magnetism of small Cr and Mn adclusters on Ni(111). This is a prototype system where two types of magnetic frustration occur: (i) frustration within the adcluster and (ii) frustration arising from antiferromagnetic coupling between the adatoms in the cluster and competing magnetic interaction between the adclusters and the surface atoms.

The triangular geometry of the Ni(111) substrate is a necessary condition for the first type of frustration. In this respect, the situation is fundamentally different from the one of Cr or Mn adclusters on Ni(001), where no compact trimers can be formed, and where thus only mechanism (ii) appears.[5] The fundamental difference is also evident from the energy gain of the emerging noncollinear state (compared to the collinear state), which is much larger in the case of the Ni(111) substrate.

While the resulting collinear and noncollinear structures are very complex, a unifying feature is that all compact structures (dimers, trimers, and tetramers) have very small total moments, as a result of the strong antiferromagnetic coupling between the cluster atoms leading to a noncollinear state with nearly complete compensation of the local mo-

ments. In most of these cases, the present local density-functional calculations give more than one energy minimum, corresponding to different noncollinear states, which are energetically very close (with differences of a few meV/atom). Thus the system can easily fluctuate between these states. However, all of them are characterized by a low total magnetic moment. On the other hand, the more open structures, like the corner and linear trimers and the tetramer *b*, have rather large total moments of about $4\mu_B$. Since the transition between a compact and an open structure requires us to move one adatom by just one atomic step, we might consider this motion as a magnetic switch, which via the local magnetic exchange field of the single adatom allows us to switch the total moment on and off, and which therefore might be of interest for magnetic storage. Thus magnetic frustration might be useful for future nanosize information storage.

ACKNOWLEDGMENT

This work was financed by the Priority Program "Clusters in Contact with Surfaces" (SPP 1153) of the Deutsche Forschungsgemeinschaft.

*Electronic address: s.lounis@fz-juelich.de

[1] J. T. Lau, A. Föhlisch, R. Nietubyć, M. Reif, and W. Wurth, Phys. Rev. Lett. **89**, 057201 (2002).

[2] P. Gambardella, S. Rusponi, M. Veronese, S. S. Dhesi, C. Grazioli, A. Dallmeyer, I. Cabria, R. Zeller, P. H. Dederichs, K. Kern, C. Carbone, and H. Brune, Science **300**, 1130 (2003).

[3] T. Jamneala, V. Madhavan, and M. F. Crommie, Phys. Rev. Lett. **87**, 256804 (2001).

[4] A. J. Heinrich, J. A. Gupta, C. P. Lutz, and D. M. Eigler, Science **306**, 466 (2004).

[5] S. Lounis, Ph. Mavropoulos, P. H. Dederichs, and S. Blügel, Phys. Rev. B **72**, 224437 (2005).

[6] S. Lounis, M. Reif, Ph. Mavropoulos, L. Glaser, P. H. Dederichs, M. Martins, S. Blügel, and W. Wurth, arXiv:cond-mat/0608048 (unpublished).

[7] R. Robles and L. Nordström, Phys. Rev. B **74**, 094403 (2006).

[8] A. Bergman, L. Nordström, A. B. Klautau, S. Frota-Pessôa, and O. Eriksson, Phys. Rev. B **73**, 174434 (2006).

[9] G. M. Stocks, M. Eisenbach, B. Újfalussy, B. Lazarovits, L. Szunyogh, and P. Weinberger, Prog. Mater. Sci. **25**, 371 (2007).

[10] H. J. Gotsis, N. Kioussis, and D. A. Papaconstantopoulos, Phys. Rev. B **73**, 014436 (2006).

[11] S. Uzdin, V. Uzdin, and C. Demangeat, Surf. Sci. **482-485**, 965 (2001); Comput. Mater. Sci. **17**, 441 (2000); Europhys. Lett. **47**, 556 (1999).

[12] A. T. Costa, R. B. Muniz, and D. L. Mills, Phys. Rev. Lett. **94**, 137203 (2005).

[13] We prefer to use the LSDA instead of the generalized gradient approximation (GGA) because self-consistent calculations are much easier to converge and because we do not expect large differences between the LSDA and GGA, as explained in Sec. VII.

[14] S. H. Vosko, L. Wilk, and M. Nusair, J. Chem. Phys. **58**, 1200 (1980).

[15] N. Stefanou, H. Akai, and R. Zeller, Comput. Phys. Commun. **60**, 231 (1990); N. Stefanou and R. Zeller, J. Phys.: Condens. Matter **3**, 7599 (1991).

[16] N. Papanikolaou, R. Zeller, and P. H. Dederichs, J. Phys.: Condens. Matter **14**, 2799 (2002).

[17] K. Wildberger, R. Zeller, and P. H. Dederichs, Phys. Rev. B **55**, 10074 (1997), and references therein.

[18] B. Drittler, M. Weinert, R. Zeller, and P. H. Dederichs, Phys. Rev. B **39**, 930 (1989).

[19] L. Nordström and D. J. Singh, Phys. Rev. Lett. **76**, 4420 (1996).

[20] I. E. Dzialoshinskii, Zh. Eksp. Teor. Fiz. **32**, 1547 (1957) [Sov. Phys. JETP **5**, 1259 (1957)]; T. Moriya, Phys. Rev. **120**, 91 (1960).

[21] I. Fischer and A. Rosch, Europhys. Lett. **68**, 93 (2004).

[22] S. Alexander and P. W. Anderson, Phys. Rev. **133**, A1594 (1964).

[23] O. Šipr, S. Bornemann, J. Minár, S. Polesya, V. Popescu, A. Šimunek, and H. Ebert, J. Phys.: Condens. Matter **19**, 096203 (2007).

[24] B. Nonas, I. Cabria, R. Zeller, P. H. Dederichs, T. Huhne, and H. Ebert, Phys. Rev. Lett. **86**, 2146 (2001); I. Cabria, B. Nonas, R. Zeller, and P. H. Dederichs, Phys. Rev. B **65**, 054414 (2002).

[25] Š. Pick, V. S. Stepanyuk, A. N. Baranov, W. Hergert, and P. Bruno, Phys. Rev. B **68**, 104410 (2003).